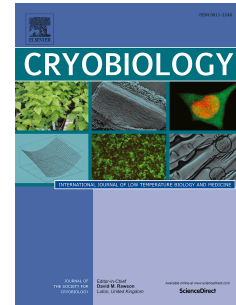


Accepted Manuscript

Convective heat transfer coefficients of open and closed Cryotop[®] systems under different warming conditions

M.V. Santos, M. Sansinena, J. Chirife, N. Zaritzky



PII: S0011-2240(18)30172-X

DOI: [10.1016/j.cryobiol.2018.08.007](https://doi.org/10.1016/j.cryobiol.2018.08.007)

Reference: YCRYO 4003

To appear in: *Cryobiology*

Received Date: 14 May 2018

Revised Date: 8 August 2018

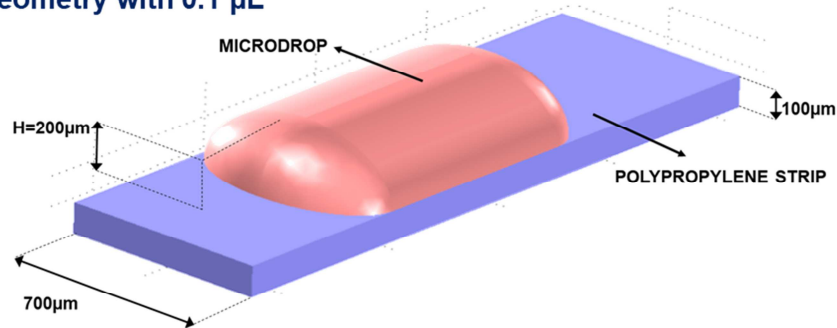
Accepted Date: 11 August 2018

Please cite this article as: M.V. Santos, M. Sansinena, J. Chirife, N. Zaritzky, Convective heat transfer coefficients of open and closed Cryotop[®] systems under different warming conditions, *Cryobiology* (2018), doi: 10.1016/j.cryobiol.2018.08.007.

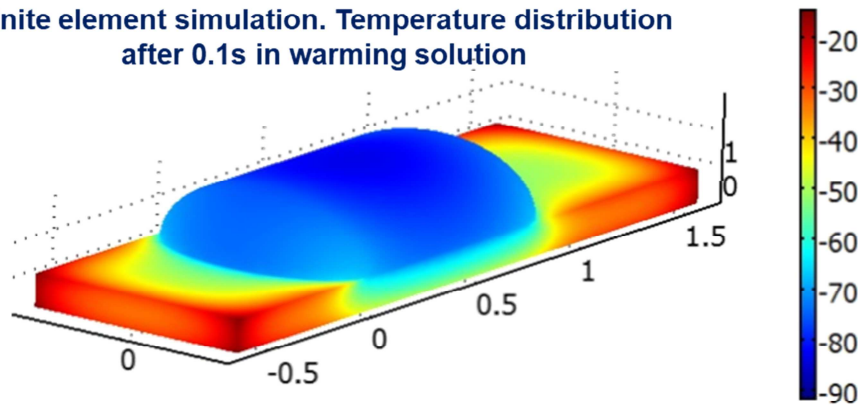
This is a PDF file of an unedited manuscript that has been accepted for publication. As a service to our customers we are providing this early version of the manuscript. The manuscript will undergo copyediting, typesetting, and review of the resulting proof before it is published in its final form. Please note that during the production process errors may be discovered which could affect the content, and all legal disclaimers that apply to the journal pertain.

GRAPHICAL ABSTRACT

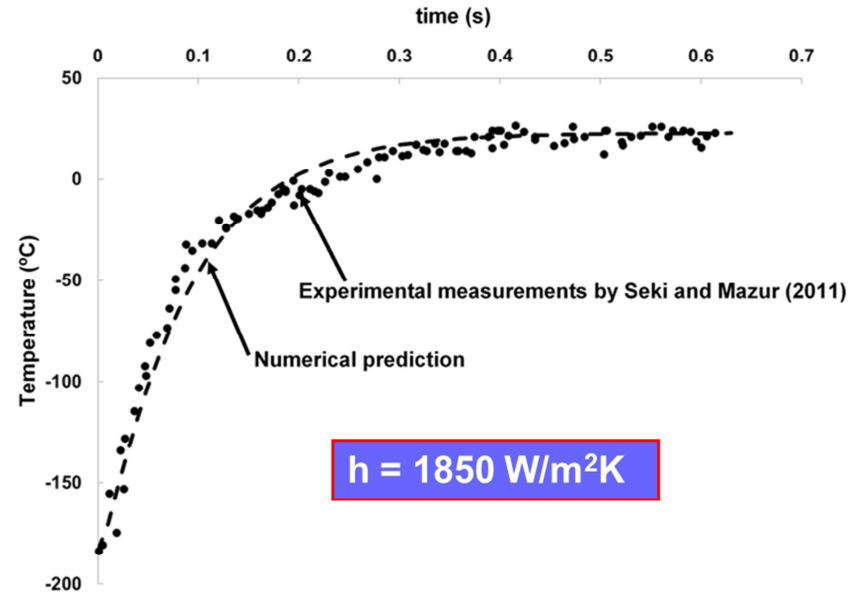
Numerical simulation of the heat transfer equation during warming of Cryotop@ system using different protocols

Geometry with 0.1 μL 

Finite element simulation. Temperature distribution after 0.1s in warming solution



Surface heat transfer coefficients $h > 1850 \text{ W/m}^2\text{K}$ that correspond to the process that achieves the highest warming rates 96000-117500 $^{\circ}\text{C}/\text{min}$

Cryotop Open System immersed in sucrose solution 23 $^{\circ}\text{C}$ 

1 **Convective heat transfer coefficients of open and closed Cryotop[®]**
2 **systems under different warming conditions**

3
4
5
6
7 M.V. Santos^{a,c*}, M. Sansinena^{b,c}, J. Chirife^b, and N. Zaritzky^{a,c}

8
9 ^aDepto. de Ingeniería Química, Facultad de Ingeniería, Universidad Nacional de La
10 Plata (Chemical Engineering Department, Faculty of Engineering, University of La
11 Plata) and Centro de Investigación y Desarrollo en Criotecnología de Alimentos
12 (Center of Research and Development of Food Cryotechnology CIDCA, CONICET-
13 UNLP-CIC PBA) , Calle 47 y 116, La Plata 1900, Argentina.

14
15 ^bFacultad de Ingeniería y Ciencias Agrarias, Pontificia Universidad Católica Argentina
16 (Faculty of Engineering and Agricultural Sciences, Pontifical Catholic University
17 Argentina), C.A.B.A., Argentina. Av. A.M. de Justo 1500, CABA (C1107AAZ),
18 Argentina.

19
20 ^cConsejo Nacional de Investigaciones Científicas y Técnicas (National Scientific and
21 Technical Research Council, Argentina). Godoy Cruz 2290, CABA 1425, Argentina.

22
23 * Corresponding author: mvsantosg@gmail.com

24

25 **Abstract**

26 The warming of cryopreserved samples supported by small volume devices is
27 governed by heat transfer phenomena which are mathematically described by the
28 solution of the transient heat conduction partial differential equations; the convective
29 heat transfer coefficient (h) is an important parameter involved in the boundary
30 condition which is related to the fluid dynamic behavior at the interface device-warming
31 fluid (water, sucrose solution or air). Unfortunately, h values for small volume devices
32 (i.e. Cryotop[®]) have not been experimentally determined. Moreover, heat transfer
33 coefficients during warming of Cryotop[®] cannot be obtained through classical
34 dimensionless correlations expressed in terms of Nusselt vs. Reynolds and Prandtl
35 numbers that are available for regular geometries and single materials.

36 It is the purpose of present work to determine the convective heat transfer coefficients
37 (h) by numerically solving the heat transfer equation applying the finite element
38 method. Numerical simulations allowed to predict time-temperature histories and
39 warming rates under different protocols in Cryotop[®] system which were compared with
40 literature warming rates reported for this device. The h values were calculated
41 considering the heterogeneous structure of the domain (microdrop, plastic-support) and
42 the irregular three-dimensional geometry. The warming conditions analyzed were: a)
43 open system in contact with air and sucrose solution at 23°C) and b) closed system in
44 contact with air and water at 23°C. The h values of the Cryotop[®] open system
45 immersed in sucrose solution (23 °C), that according to literature achieved a survival in
46 the order of 80%, are in the range of 1800 to 2200 W/m²K. The h values obtained in
47 this work for warming conditions are critical parameters for cryobiologists when
48 studying heat transfer rate in this small volume device.

49 Keywords: numerical simulation; vitrification; warming rates; surface heat transfer
50 coefficient; Cryotop[®]

51

ACCEPTED MANUSCRIPT

52 INTRODUCTION

53 Thermal histories during cooling, storage, and warming are fundamental aspects
54 that critically influence the cryosurvival of reproductive cells. Vitrification has become
55 the method of choice for low temperature preservation of large-volume cells such as
56 oocytes and embryos and has replaced equilibrium freezing in most clinical settings
57 [5,6,14]. This phenomenon is a non-equilibrium process in cryoprotective solutions
58 (CPS) which suppresses ice crystal formation while achieving an amorphous state.
59 Because these solutions usually contain permeating cryoprotectants with varying
60 degrees of cytotoxicity [25], multiple exposure steps and high cooling rates
61 ($>10,000^{\circ}\text{C}/\text{min}$) are necessary in order to avoid osmotic effects while reducing
62 exposure time to minimize toxicity; cells are typically loaded with minimal volume onto
63 vitrification supports and plunged in liquid nitrogen. Minimal volume systems such as
64 the Cryotop[®] have been shown to achieve these high cooling rates [12].

65 Studies of different vitrification carrier systems have mostly focused on the cooling
66 process and the quantification of the cooling rates necessary to achieve vitrification.
67 However, several works proposed that the warming rate of vitrified samples might be
68 the most important factor that determines cell cryosurvival [13, 20, 21]. The work by
69 Seki and Mazur [22] was the first report which showed the dominant effect of warming
70 rate over cooling rate on the survival of mouse oocytes, and was later corroborated
71 specifically for Cryotop[®] in 2012 [23]. Their results indicated that, irrespective of
72 cooling rate, murine oocyte survival was 70-85% when warming was performed at the
73 highest rate (96,000-117,000 $^{\circ}\text{C}/\text{min}$) [23]. In this study, the authors measured the time-
74 temperature histories during cooling and warming of a sample mounted on Cryotop[®]
75 using a 50 μm copper-constantan thermocouple, and recorded data with a computer-
76 oscilloscope. This simple experimental procedure allowed for the quantification of the
77 warming rates achieved in a Cryotop[®] under several operating conditions.

78 The Cryotop[®] is a heterogeneous system consisting of a fine polypropylene strip
79 supporting the micro-drop of the biological sample. The whole system is a complex
80 irregular three-dimensional domain with materials of different thermophysical properties
81 that cannot be assimilated to a simple regular geometry of a homogeneous material.

82 The warming process of cryopreserved samples is governed by heat transfer
83 phenomena that can be mathematically described by the solution of the transient heat
84 conduction partial differential equations. The time-temperature histories and warming
85 rates in cryo-devices under different protocols can be predicted by numerical
86 simulations of these partial differential equations that must be experimentally validated.
87 The finite element method (FEM) is a powerful technique originally developed for the
88 numerical solution of complex problems in structural mechanics, it has been
89 extensively applied in many engineering problems that involve mass and energy
90 transfer. In order to simulate heat transfer in Cryotop[®] and predict time temperature
91 curves, FEM is considered the method of choice since it can deal with the high level of
92 complexity encountered in this type of systems: irregular geometry and heterogeneous
93 domain of the device.

94 The application of mathematical models requires the knowledge of the
95 thermophysical properties of the biological fluid and the plastic support material. In the
96 past, authors have used equilibrium thermophysical properties that considered the
97 presence of ice for cell suspensions; however, vitrification is a non-equilibrium process
98 which requires specific properties.

99 The surface heat transfer coefficient (h) is an important parameter involved in the
100 boundary condition which is related to the fluid dynamic behavior at the interface
101 device-warming fluid (water and/or air). Numerical calculations of warming rates require
102 the knowledge of accurate h values that will predict the performance of a specific
103 cryobiological procedure. Heat transfer coefficients during warming of Cryotop[®] system
104 cannot be obtained using classical dimensionless correlations expressed in terms of

105 Nusselt vs. Reynolds and Prandtl numbers that are available for regular geometries
106 and single materials. In order to determine the h values that represent the warming
107 rates of each protocol heat transfer numerical solutions must be compared with
108 experimental time- temperature measurements. Santos et al. [18, 19] have reported
109 surface heat transfer coefficients in several cryopreservation systems (plastic French
110 straws, Cryoloop[®], Cryotop[®], OPS among others) in order to estimate the performance
111 of different cooling protocols and procedures (direct plunging in liquid nitrogen or
112 freezing in nitrogen vapor).

113 Information about convective heat transfer coefficients during the warming process
114 of Cryotop[®] have not yet been reported in literature; however, these coefficients are
115 needed for the optimization of warming protocols [26] .

116 The main objective of the present study was to determine heat transfer coefficients
117 during warming using Cryotop[®] systems under different conditions, while considering
118 the effects of the thermophysical properties and the loading volume. The warming
119 conditions included in the analysis are: a) Cryotop[®] (open system in contact with air
120 and sucrose solution at 23°C), b) Cryotop[®] (closed system in contact with air and
121 water at 23°C).

122

123 **MATERIALS AND METHODS**

124 ***Vitrification system***

125 The Cryotop[®] vitrification carrier, consists of a fine strip of polypropylene
126 transparent film of 0.7 mm wide, 20 mm long and 0.1 mm thick [23, 10], attached to a
127 plastic handle resistant to liquid nitrogen. It is interesting to note that in different
128 publications [11, 12, 13] a strip width of 0.4mm was reported, however the actual value
129 is 0.7mm (Fig.1)

130 The polypropylene tip has a flat film area where a minimal volume can be loaded
131 (0.1-0.2 μL containing 4-8 oocytes or embryos) and subsequently plunged into liquid
132 nitrogen. The Cryotop[®] allows for a sample to be cooled at a very high rate in order to
133 achieve vitrification. Samples can be vitrified either in direct contact with liquid nitrogen
134 (open system) or contained within a protective cap that isolates the loaded sample from
135 the cryogenic fluid (closed system, Cryotop[®] SC Kitazato Supply, Inc, JP). Once
136 vitrified, the warming protocols have been shown by Mazur and Seki (2011) to be a key
137 aspect of cell survival.

138

139 **NUMERICAL MODELING**

140 ***Cryotop[®] dimensions and geometry. Support material***

141 The geometry of the Cryotop[®] system used for the heat transfer numerical
142 simulation was based on the information published by Jin et al. [10] and Seki and
143 Mazur [23]. The two domains (microdrop and polypropylene strip) are shown in Figure
144 1. Besides the position of the thermocouple junction used by Kleinhans et al. [11]
145 whose experimental measurements were simulated in the present work are also shown
146 Fig.1. The selected point corresponding to the thermocouple position has the following
147 spatial coordinates: $x=110\mu\text{m}$, $y=0$, $z=126\mu\text{m}$ (Fig. 1).

148 The spatial discretization of the 3D domains was implemented using tetrahedral and
149 triangular elements for the inner and boundary domains, respectively (Fig.1). The
150 Cryotop[®] protocol requires the minimal volume droplet to be carefully spread into a thin
151 film over the plastic polypropylene strip. Two different drop volumes (0.1 and 0.2 μL)
152 were simulated in order to study the effect of the loaded microdrop on the warming
153 rate. In Fig. 1 the height of the droplet (H) corresponds to 0.1 μL droplet volume.

154 The warming modeling conditions selected for the present study (Figure 2) were
 155 based on earlier reports by Mazur and Seki (2011)[13], in which warming rates were
 156 experimentally measured.

157

158 ***Mathematical modeling of heat transfer***

159 The partial differential equations that represent conductive heat transfer in the
 160 Cryotop[®] system (negligible convective contribution) during warming can be described
 161 as a 3D problem using Cartesian coordinates:

$$162 \quad \rho_s C p_s \frac{\partial T}{\partial t} = -\nabla \cdot (-k_s \nabla T) \quad \text{at} \quad \Omega 1$$

163 (1)

$$164 \quad \rho_p C p_p \frac{\partial T}{\partial t} = -\nabla \cdot (-k_p \nabla T) \quad \text{at} \quad \Omega 2$$

165 (2)

166

167 where T is temperature, ρ is the density, C_p specific heat, k thermal conductivity.
 168 The effect of temperature on the thermo-physical properties of the biological solution
 169 were considered.

170 The subscript \underline{s} corresponds to the domain $\Omega 1$ (droplet of biological solution) and \underline{p}
 171 to the plastic material ($\Omega 2$)

172 The initial temperature condition was considered uniform in both material domains.

$$173 \quad T_0 = -196^\circ\text{C} \quad \text{at} \quad t = 0 \quad \text{for} \quad \Omega 1 \quad \text{and} \quad \Omega 2 \quad (3)$$

174 According to the simulated warming protocols (Figure 2) the convective boundary
 175 conditions for the plastic support and for the microdroplet in contact with the external
 176 media (air or liquid warming medium) are expressed as follows:

$$177 \quad -k_p \nabla T \cdot \mathbf{n} = h (T - T_{\text{ext}}) \quad \text{at} \quad \partial \Omega 1$$

178 (4)

$$179 \quad -k_s \nabla T \cdot \underline{n} = h (T - T_{\text{ext}}) \quad \text{at} \quad \partial\Omega_2$$

180 (5)

181 where, h is the average surface heat transfer coefficient at $\partial\Omega_1$ (interface of the
 182 plastic strip) and $\partial\Omega_2$ (interface of the droplet); T is the variable surface temperature of
 183 the microdroplet or the plastic strip exposed to the external medium; T_{ext} is the external
 184 temperature and its value depends on the protocol used as warming process, \underline{n} is the
 185 normal outward vector.

186 The heat transfer resistance of the closed Cryotop[®] (with a cap) is given by the sum
 187 of several serial heat transfer resistances: air insulation, the thickness of the plastic cap
 188 and the external fluid which can be air or water.

189 It is interesting to note that Kleinhans et al. [11] measured the response of a Cryotop
 190 system with includes a thermocouple as part of the mass to be warmed. These authors
 191 estimated that the heat capacity of the thermocouple represented only 5% of the total
 192 thermal mass. Therefore in the present work the influence of the thermocouple was
 193 considered negligible

194 The differential equations (1)-(5) that represent the warming process were
 195 numerically solved using the finite element method in COMSOL 3.5 AB Multiphysics
 196 (lic. 1048485).

197

198 ***Thermophysical properties***

199 The thermophysical properties used in the model (specific heat, thermal conductivity
 200 and density) of the polypropylene strip, ice and vitrified water are summarized in Table
 201 1 for the temperature range -196 to 0°C

202 There is a wide range of biological formulations used for cryopreservation purposes
 203 that vary in terms of the type of cryoprotective agents incorporated.

204 The thermal properties therefore are important parameters that must be carefully
 205 selected to simulate heat transfer phenomena and these properties depend on both the

206 protocol (warming rate) which is related to the volume load of the sample and the
207 proximate composition of the biological solution.

208 Ehlich et al. [7] experimentally determined the thermal conductivity of water-DMSO
209 solutions using the hot wire technique; results showed that in a DMSO solution ranging
210 between 2 and 6 M crystallization occurs and the thermal conductivity increases as the
211 temperature decreases. In contrast, above approximately 7.05 M DMSO vitrification
212 occurs and the thermal conductivity is independent of the concentration of solutes and
213 of temperature. The presence or absence of ice was observed in the experiments using
214 cryomicroscope images. Choi and Bischof [3] have also reported thermophysical
215 properties (k , ρ , C_p) of biologically relevant solutions, liquids, and tissues that are
216 important in the cryobiology field.

217 If the warming rate is sufficiently high to avoid recrystallization or devitrification, then
218 the thermophysical properties of a vitreous biological solution should be applied. On
219 the contrary, when the warming rates are low and there is a partial or total
220 crystallization of ice, then thermophysical properties under equilibrium conditions
221 should be applied. In the last case, the use of Differential Scanning Calorimetry can be
222 helpful for the estimation of thermal properties such as specific heat (C_p) which is
223 strongly temperature dependent.

224 Due to the scarce information concerning the thermophysical properties of the
225 specific biological fluid used by Mazur and Seki [13] a simplification was implemented
226 using thermophysical properties of ice (for low warming rates) or vitrified water (for high
227 warming rates) instead of the actual values of the biological complex systems.

228 The implementation of these properties has been previously applied for numerical
229 simulations of the performance of several vitrification devices [16].

230 For an open Cryotop[®] system directly immersed in a 23°C solution, the warming
231 rate corresponds to the highest value (96,000-117,000°C/min) that allowed to achieve
232 the highest oocyte survival independent of the cooling rate applied [13].

233 Therefore, in this scenario, the numerical model applied in the present work was
234 that of vitreous water; the thermophysical properties as a function of temperature are
235 shown in Table 1.

236 In the case of other simulated protocols with lower warming rates, partial formation
237 of ice due to recrystallization or devitrification phenomena could be responsible for the
238 observed decrease in survival rates [13, 17]. Therefore, in the present work, one set of
239 simulations were carried out considering the thermophysical properties of ice and
240 another set assuming vitreous water, in order to find the range of surface heat transfer
241 coefficients that describe the warming process. In addition, the effect of varying these
242 properties on the h values calculated were assessed. The thermophysical properties of
243 ice which were considered dependent on temperature in the numerical model are also
244 shown in Table 1.

245

246 ***Warming simulations under different conditions.***

247 Table 2 shows the simulated warming conditions for which the surface heat transfer
248 coefficients were calculated.

249 Mazur and Seki [13] measured the time-temperature curves during warming
250 protocols consisting in the exposure of a closed Cryotop[®] system (CS) to an external
251 temperature of 23°C in air and in a liquid warming media (water or sucrose solution). In
252 the case of the open Cryotop[®] (OS) system, the experiments were carried out with
253 immediate immersion into a liquid warming media or in air both at 23°C.

254 In the case of the open Cryotop[®] with direct immersion in warming solution at 23°C
255 Mazur and Seki [13] reported the entire time-temperature data. The numerical FEM
256 was applied by varying the h value and then comparing the predicted time- temperature
257 curve with the experimental curve reported by the authors. The heat transfer coefficient
258 that minimized the absolute error of the temperature history was selected.

259 For the other protocols (P2, P3, and P4) time-temperature data are not available;
260 only warming rates were reported, therefore the numerical FEM was applied to
261 estimate the surface heat transfer coefficients (h) by comparing the experimental
262 warming rates with the predicted ones obtained through the numerical thermal histories
263 calculated by the model. The heat transfer coefficient that minimized the absolute error
264 of the warming rates was selected. Mazur and Seki [13] defined the warming rate as
265 the initial straight slope of their experimental temperature - time curves before the
266 warming rate starts to slow down (from -170°C to -30°C).

267

268 **RESULTS AND DISCUSSION**

269 ***Surface heat transfer coefficients during warming under different operating*** 270 ***conditions***

271 **Protocol 1. Open Cryotop[®] immersed in sucrose solution**

272 Figure 3 shows the numerical simulations considering a volume load of $0.1\ \mu\text{L}$ and
273 vitreous water. The h value that best fitted experimental data was $1850\text{W}/\text{m}^2\text{K}$; as can
274 be observed there is an excellent agreement between predicted and experimental
275 curves which allows the determination of the h value that represents the warming
276 process under vitreous conditions. The same numerical procedure was applied with a
277 volume load of $0.2\ \mu\text{L}$ and the h calculated value was $2200\text{W}/\text{m}^2\text{K}$. These values are
278 representative of the range of h that generate a warming rate of $96,000^{\circ}\text{C}/\text{min}$. As was
279 mentioned before the h values cannot be estimated by the dimensionless Nusselt
280 correlations. The numerical finite element program allowed to obtain the time-
281 temperature distribution at any point inside the domains as time elapses.

282 A tetrahedral mesh using Lagrange elements of order 2 was applied to discretize the
283 domains. The number of elements that constituted the mesh for the microdroplet with
284 different volumes and plastic support are shown in Table 3. The time discretization

285 scheme used was a Backward Euler Differentiation (minimum order 1 and maximum
286 order 5) with a tuning step having a maximum of 0.1 s and a minimum initial starting
287 value of 0.001s. The absolute and relative tolerances for each integration step were
288 0.001 and 0.01, respectively.

289 All the numerical runs were tested for their computational speed, the maximum CPU
290 time was less than 5 min for the 3D model runs using a PC Intel(R) Core(TM) i3 6300
291 with a processor speed of 3.80 GHz and a RAM of 4 GB.

292 Figure 4 a, b shows the numerical simulations and time-temperature distribution in
293 the whole system with the inner views at different positions.

294 The values of h determined in the present work for the Protocol 1, that achieved a
295 survival in the order of 80 % according to Mazur and Seki (2011) are in the range
296 1800 to 2200 W/m²K which are higher than expected for different solids such as thin
297 plates or small cylinders immersed in stagnant fluids (represented by sucrose
298 solution). These high values may indicate nucleate boiling of the liquid nitrogen that is
299 moistening or in intimate contact adhered to the surface of the open Cryotop[®] system
300 (PP strip and droplet). This liquid film generates nitrogen vapor and bubbles when it
301 comes into contact with the warm solution that rapidly escape from the warming media
302 (it must be taken into account that LN2 boils at -196°C at atmospheric pressure). This
303 phenomenon is commonly observed when a cryobiological device coming from a liquid
304 nitrogen container is rapidly immersed in a warming solution. The nitrogen bubbles that
305 escape from the device generate a fluid dynamic pattern that is far from the stagnant
306 conditions, leading to higher h values. Another possible source of convective
307 contribution can be originated by the laboratory operator through the swirling of the
308 Cryotop[®] to homogenize temperature profiles.

309

310 **Warming protocols of open and closed Cryotop[®] immersed in water and air.**

311 Table 4 shows the heat transfer coefficients and warming rates predicted with the
312 numerical simulations of the Cryotop[®] under different conditions and using
313 thermophysical properties for both glassy water and ice.

314 As can be observed the h values at the lowest possible warming rates (Protocol 4,
315 Cryotop[®] closed system warmed in air) correspond to an external and internal
316 stagnant fluid (air inside and outside the cap of the Cryotop[®]). The volume loaded on
317 the Cryotop[®] for this protocol did not influence the low h value ($h=5.5 - 6.5 \text{ W/m}^2\text{K}$). As
318 was mentioned previously, the h value for the Cryotop[®] with cap is in fact a global heat
319 transfer coefficient, because it takes into account the sum of in series individual
320 resistances given by: air insulation, the thickness of the plastic cap, and the external
321 fluid. In this protocol (P4) in which the presence of air led to low heat transfer rates,
322 there is a high possibility of ice formation due to devitrification or recrystallization;
323 therefore, simulations were carried out introducing the thermal properties of ice.

324 In order to analyze the effect of the thermophysical properties on h values during
325 warming, simulations of P4 using glassy water properties were also conducted.
326 Obtained results showed that there was not an appreciable difference between the h
327 values using both set of properties: $h=5.5-6.5 \text{ W/m}^2\text{K}$ for glassy water and $h=5.5 -6$
328 $\text{W/m}^2\text{K}$ for ice.

329 The radiation heat transfer was calculated for this Protocol according to the method
330 proposed by Geankoplis [8] and the obtained value of h for radiation was $1.98 \text{ W/m}^2 \text{ K}$.
331 This value implies that there is a significant contribution of radiation to the total heat
332 transfer during the warming process.

333 Table 4 shows that thermophysical properties and the volume loaded did not affect
334 in a significant manner the warming rate. In terms of finding the bottleneck of the
335 warming process it can be concluded that in the case of Protocol 4 there is an external
336 heat control of the system, therefore the process is governed by the thermal resistance
337 of the external fluid (air).

338 When the Protocol 3 (Cryotop[®] closed system warmed in water) is used, the
339 external control decreased compared to Protocol 4 since water as immersion warming
340 fluid allows a higher heat transfer rate. Additionally, if the closed Cryotop[®] is swirled,
341 the movement of the water solution generates convective conditions. For Protocol 3 h
342 values ranged between 40 and 50 W/m²K when ice properties were used in the
343 simulations and higher values of h (53-60 W/m²K) were obtained when glassy water
344 properties were introduced in the model.

345 In the case of Protocol 2, an Open Cryotop[®] in contact with air was simulated
346 obtaining higher h values (>90 W/m² K) when compared to typical values of h in
347 stagnant air and to Protocol 3 (closed Cryotop[®] immersed in water). This result can be
348 attributed to the fact that the liquid nitrogen film adhered to the Cryotop[®] device
349 evaporates when it is exposed to the warm air. Nitrogen vapor released from the
350 sample produced a higher convective flow that led to higher h values. The individual
351 contribution of radiation to the total rate of heat transfer was calculated resulting in less
352 than 3%.

353

354 CONCLUSIONS

355 Surface heat transfer coefficients (h) under different warming protocols for Cryotop[®]
356 systems were estimated using numerical finite element simulations considering the
357 irregular 3D shape and the heterogeneous structure. Four warming protocols were
358 simulated: a) Cryotop[®] open system immersed in air and sucrose solution at 23°C; b)
359 Cryotop[®] closed system in direct contact with air and water at 23°C.

360 Time-temperature curves and warming rates were predicted and compared with
361 published experimental data. Numerical simulations using different volume loads and
362 thermophysical properties associated to non-equilibrium warming (glassy water) or

363 equilibrium conditions (that generates ice crystals formation or devitrification) allowed
364 to analyze the mechanisms governing the heat transfer rate for each Protocol.

365 The h values of the Cryotop[®] open system immersed in sucrose solution at 23 °C
366 (Protocol 1), that achieved a survival in the order of 80 % according to Mazur and Seki
367 (2011) are in the range of 1800 to 2200 W/m²K. Lower h values were observed for the
368 other simulated warming protocols with a lower dependence on the loaded volume and
369 thermophysical properties of the simulated fluid (ice or glassy water).

370 The h values obtained in this work for warming conditions are critical parameters for
371 cryobiologists when studying technologies associated with vitrification systems, and
372 limited information about these values are found in literature.

373 The present work contributes to the calculation of h values that represent the heat
374 transfer rate during warming of vitrified samples which might be one of the limiting
375 steps in cell survival.

376

377

378 **Conflict of interest**

379 Authors declare no conflict of interest in the present study

380

381 **Funding**

382 This study was supported by Grants obtained by the following institutions: Facultad de
383 Ingeniería y Ciencias Agrarias, Pontificia Universidad Católica Argentina; Centro de
384 Investigación y Desarrollo en Criotecnología de Alimentos (CIDCA-CONICET-CIC
385 PBA); Universidad Nacional de La Plata; CONICET; Agencia Nacional de Promoción
386 Científica y Tecnológica, Argentina.

387 **Acknowledgments**

388 We thank the following institutions: Facultad de Ingeniería y Ciencias Agrarias,
389 Pontificia Universidad Católica Argentina; Centro de Investigación y Desarrollo en
390 Criotecnología de Alimentos (CIDCA-CONICET-CIC PBA); Universidad Nacional de La
391 Plata; CONICET; Agencia Nacional de Promoción Científica y Tecnológica, Argentina.
392 Authors have expressed no conflict of interest or financial affiliation with any
393 commercial cryopreservation supports compared in the study.

394

395

396 **FIGURE CAPTIONS**

397

398 **Figure 1.** a) Cryotop[®] system (microdrop on top of the fine polypropylene strip) with a
399 volume of 0.1 μL . Spatial representation of the irregularly shaped body using
400 tetrahedral and triangular elements. Location of the thermocouple defined using the
401 photograph published by Kleinhans et al. [11] whose thermal history was simulated in
402 the present work.

403

404 **Figure 2.** Warming protocols modeled in the present study using open and closed
405 Cryotop[®].

406

407 **Figure 3.** Time- temperature measurements adapted from Kleinhans et al. [11] and
408 numerical prediction for the warming process in an Open Cryotop[®] system by
409 immersion in a sucrose solution at 23°C. Experimental warming rate of 96000°C/min.

410

411 **Figure 4.** Temperature distribution after 0.1s at :a) the external surface of the droplet
412 and PP strip, b) inner points of the microdrop at different consecutive slices in the axial
413 direction, considering a volume load of 0.1 μL , initial temperature of -196°C,
414 $h=1100\text{W}/\text{m}^2\text{K}$, and a warming solution (sucrose) at a temperature of 23°C.

415

416 REFERENCES

- 417 [1] O. Andersson, A. Inaba, Thermal conductivity of crystalline and amorphous ices
418 and its implications on amorphization and glassy water, *Phys. Chem. Chem.*
419 (2005), 1441-1449.
- 420 [2] C. A. Angell, Glass-Forming Properties Insights into Phases of Liquid Water from
421 Study of Its Unusual Glass-Forming Properties, *Science* 319 (2008) 582.
- 422 [3] J. Choi, J.C. Bischof, Review of biomaterial thermal property measurements in
423 the cryogenic regime and their use for prediction of equilibrium and non-
424 equilibrium freezing applications in cryobiology, *Cryobiology* 60 (2010) 52–
425 70.
- 426 [4] P.G. Debenedetti, H.E. Stanley, Supercooled and Glassy Water, *Journal of*
427 *Physics: Condensed Matter*, Volume 15, Number 45 (2003).
- 428 [5] I.P. Dike, Efficiency of intracellular cryoprotectants on the cryopreservation of
429 sheep oocytes by controlled slow freezing and vitrification techniques,
430 *Journal of Cell and Animal Biology*, 3 (2009) 44-49.
- 431 [6] V.H. Do, S. Walton, S. Catt, A.W. Taylor-Robinson, Improvements to in vitro
432 culture media for use in bovine IVF, *Journal of Veterinary Science & Animal*
433 *Husbandry*, 4 (1) (2016) 1-8.
- 434 [7] L.E. Ehrlich, J.S.G. Feig, S.N. Schiffres, J.A. Malen, Y. Rabin, Large Thermal
435 Conductivity Differences between the Crystalline and Vitrified States of
436 DMSO with Applications to Cryopreservation, *PLoS ONE* 10 (5) (2015).
- 437 [8] C.J. Geankoplis, *Transport processes and unit operations*, 3rd ed., Englewood
438 Cliffs, New Jersey, 1993.
- 439 [9] IAPWS, *The International Association for the Properties of Water and Steam.*
440 R10-06 (2009)
- 441 [10] B. Jin, F.W. Kleinhans, P. Mazur, Survivals of mouse oocytes approach 100%
442 after vitrification in 3-fold diluted media and ultra-rapid warming by an IR laser
443 pulse. *Cryobiology* 68 (2014) 419–430.
- 444 [11] F.W. Kleinhans, S. Seki, P. Mazur, Simple inexpensive attainment and
445 measurement of very high cooling and warming rates, *Cryobiology* 61 (2010)
446 231–233.
- 447 [12] M. Kuwayama, G. Vajta, O. Kato, S.P. Leibo, Highly efficient vitrification method
448 for cryopreservation of human oocytes, *Reprod Biomed Online* 11 (3) (2005)
449 300-308.
- 450 [13] P. Mazur, S. Seki, Survival of mouse oocytes after being cooled in a vitrification
451 solution to -196°C at 95° to $70,000^{\circ}\text{C}/\text{min}$ and warmed at 610° to
452 $118,000^{\circ}\text{C}/\text{min}$: A new paradigm for cryopreservation by vitrification,
453 *Cryobiology*, 62 (2011) 1-7.
- 454 [14] S.F. Mullen, M. Li, Y. Li, Z.J. Chen, J.K. Critser, Human oocyte vitrification: The
455 permeability of metaphase II oocytes to water and ethylene glycol and the
456 appliance toward vitrification, *Fertil Steril.* 89(6) (2008) 1812–1825.
- 457 [15] V. F. Petrenko, R. W. Whitworth, *Physics of ice*, Oxford University Press,
458 Oxford, 1999.
- 459 [16] M. Sansinena, M.V. Santos, N. Zaritzky, J. Chirife, Numerical simulation of
460 cooling rates in vitrification systems used for oocyte cryopreservation,
461 *Cryobiology* 63 (2011) 32-37.
- 462 [17] M. Sansinena, M.V. Santos, J. Chirife, N. Zaritzky, In-vitro development of
463 vitrified–warmed bovine oocytes after activation may be predicted based on
464 mathematical modelling of cooling and warming rates during vitrification,
465 storage and sample removal, *Reprod. BioMedicine Online* 36 (2018) 500-507.
- 466 [18] M.V. Santos, M. Sansinena, J. Chirife, N. Zaritzky. Determination of heat
467 transfer coefficients in plastic French straws plunged in liquid nitrogen.
468 *Cryobiology* 69 (2014), 488–495.

- 469 [19] M.V. Santos, M. Sansinena, N. Zaritzky, J. Chirife, Experimental determination
470 of surface heat transfer coefficient in a dry ice-ethanol cooling bath using a
471 numerical approach, *Cryoletters* 38 (2) (2017).
- 472 [20] S. Seki, B. Jin, P. Mazur, Extreme rapid warming yields high functional survivals
473 of vitrified 8-cell mouse embryos even when suspended in a half-strength
474 vitrification solution and cooled at moderate rates to -196 C. *Cryobiology* 68
475 (2014) 71–78.
- 476 [21] S. Seki, P. Mazur, Effect of Warming Rate on the Survival of Vitrified Mouse
477 Oocytes and on the Recrystallization of Intracellular Ice, *Biology of*
478 *Reproduction* 79 (2008) 727–737.
- 479 [22] S. Seki, P. Mazur, The dominance of warming rate over cooling rate in the
480 survival of mouse oocytes subjected to a vitrification procedure, *Cryobiology*
481 59 (2009) 75-82.
- 482 [23] S. Seki, P. Mazur, Ultra-Rapid Warming Yields High Survival of Mouse Oocytes
483 Cooled to -196°C in Dilutions of a Standard Vitrification Solution. *PLoS ONE*
484 7 (4) (2012) e36058.
- 485 [24] M. Sugisaki, H. Suga, S. Seki, Calorimetric Study of the Glassy State. IV. Heat
486 Capacities of Glassy Water and Cubic Ice. *Bulletin of the Chemical Society of*
487 *Japan* 41 (1986) 2591-2599.
- 488 [25] C.A. Van de Voort, C.R. Shirley, D.N. Hill, S.P. Leibo. *Fertility and Sterility*, 90
489 (2008) 805-816
- 490 [26] T. Wang, G. Zhao ,H.Y. Tang,Z.D. Jiang, Determination of convective heat
491 transfer coefficient at the outer surface of a cryovial being plunged into liquid
492 nitrogen, *CryoLetters* 36(2015), 285-288.
- 493

Table 1 . Effect of temperature on thermophysical properties used in the simulations

Materials	Thermophysical properties			
	k (W/m ² K)	ρ (Kg/m ³)	Cp (J/kg K)	References
Polypropylene	0.22 (-196°C , 23°C)	920 (-196°C , 23°C)	1900 (-196°C , 23°C)	[11]
Glassy Water	1.1 (-196°C , 23°C)	940 (-196°C , 23°C)	1078.88 (-154.18 °C) 1120.55 (-150.77 °C) 1173.33 (-146.83 °C) 1216.11 (-142.99 °C)	[1, 2, 4, 24]
Ice	2.22 (0 °C) 2.25 (-5 °C) 2.3 (-10 °C) 2.34 (-15 °C) 2.39 (-20 °C) 2.45 (-25 °C) 2.5 (-30 °C) 2.57 (-35 °C) 2.63 (-40 °C) 2.76 (-50 °C) 2.9 (-60 °C) 3.05 (-70 °C) 3.19 (-80 °C) 3.34 (-90 °C) 3.7 (-100 °C) 4.1 (-110 °C) 4.3 (-120 °C) 4.7 (-130 °C) 5.2 (-140 °C) 5.6 (-150 °C) 6 (-180 °C)	917.2 (0 °C) 924.13 (-50 °C) 929.3 (-100 °C) 931.0 (-150 °C)	2100 (0 °C) 1967 (-20 °C) 1833 (-40 °C) 1700 (-60 °C) 1566 (-80 °C) 1433 (-100 °C)	[3, 9, 7, 15]

Table 2. Warming protocols simulated using FEM for different droplet volumes (0.1 and 0.2 μL)

<i>Warming Protocol</i>	<i>Cryotop[®] System</i>	<i>Description</i>
P1	Open	Sucrose solution (23°C)*
P2	Open	Holding in Air (23°C)
P3	Closed	Immersion in water (23°C)
P4	Closed	Holding in Air (23°C)

*0.5 M sucrose solution

Table 3. Dimensions of the droplets and mesh parameters

	Mesh parameters		
	N° Tetrahedral elements (domain)	N° Triangular elements (boundary)	Total node points
Cryotop with 0.1 μL H= 200 μm^*	20232	3642	4426
Cryotop with 0.2 μL H= 280 μm^*	12162	2516	2735

*H= height of the droplet according to the volume loaded (See Fig. 1)

TABLE 4. Convective heat transfer coefficients (h), experimental warming rates and predicted values using numerical simulations of the Cryotop® system under different warming protocols, droplet volumes and thermophysical properties of the simulated fluid (ice or glassy water).

Warming Protocol Cryotop®	Simulated fluid	Droplet volume loaded (μL)	Heat transfer coefficients h (W/m ² K)	Predicted warming rate using FEM (°C/min)	Experimental warming rate (Mazur and Seki, 2011) (°C/min)
P2 OPEN in air	Ice	0.1	90	7758	7850 ± 415
		0.2	110	7828	
	Glassy Water	0.1	120	7845	
		0.2	140	7868	
P3 CLOSED with cap in water	Ice	0.1	40	3985	4050 ± 328
		0.2	50	4033	
	Glassy Water	0.1	53	4157	
		0.2	60	4034	
P4 CLOSED with cap in air	Ice	0.1	5.5	642	612 ± 40
		0.2	6	618	
	Glassy Water	0.1	5.5	618	
		0.2	6.5	630	

FIGURE 1. BLACK AND WHITE

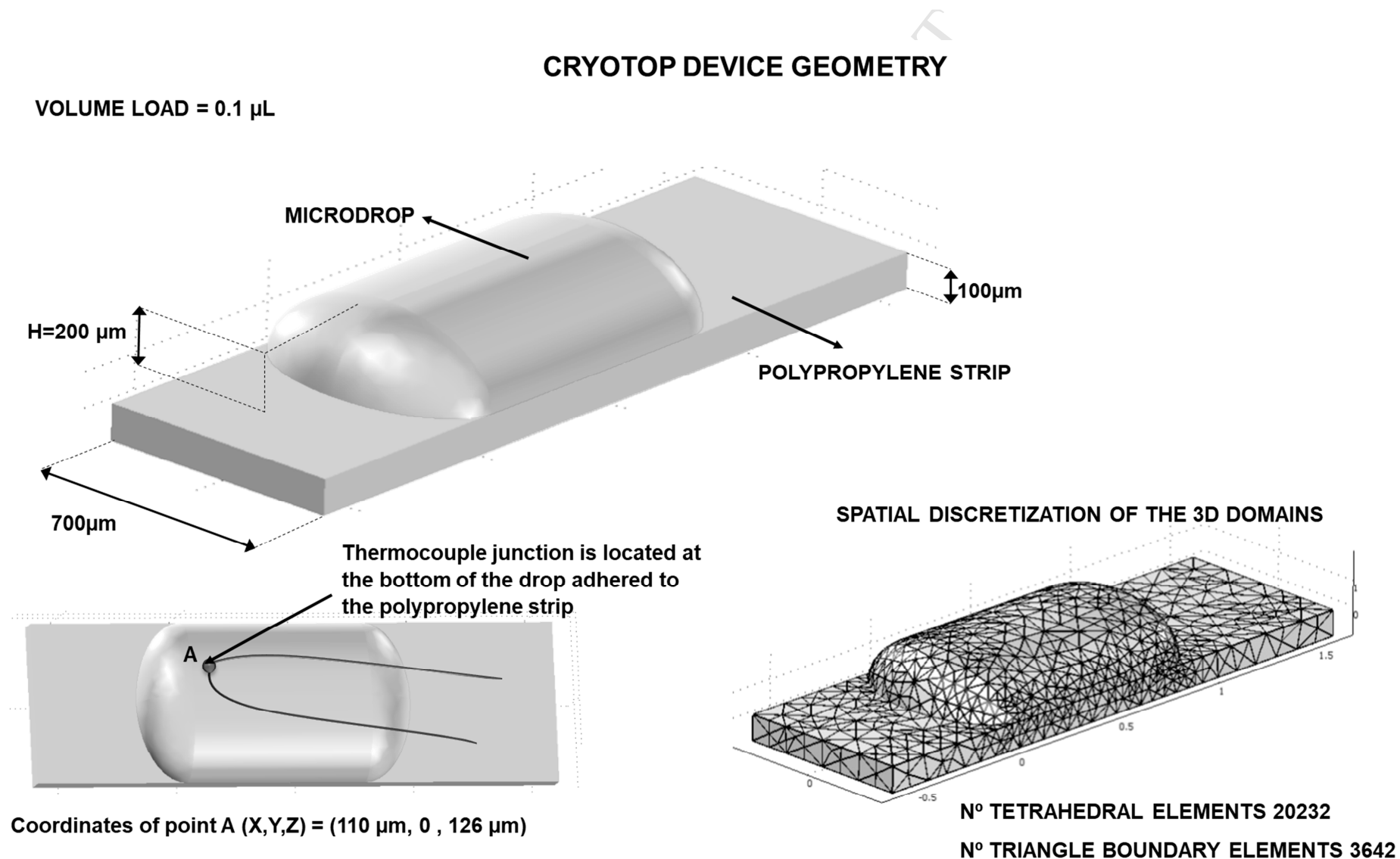


FIGURE 1.

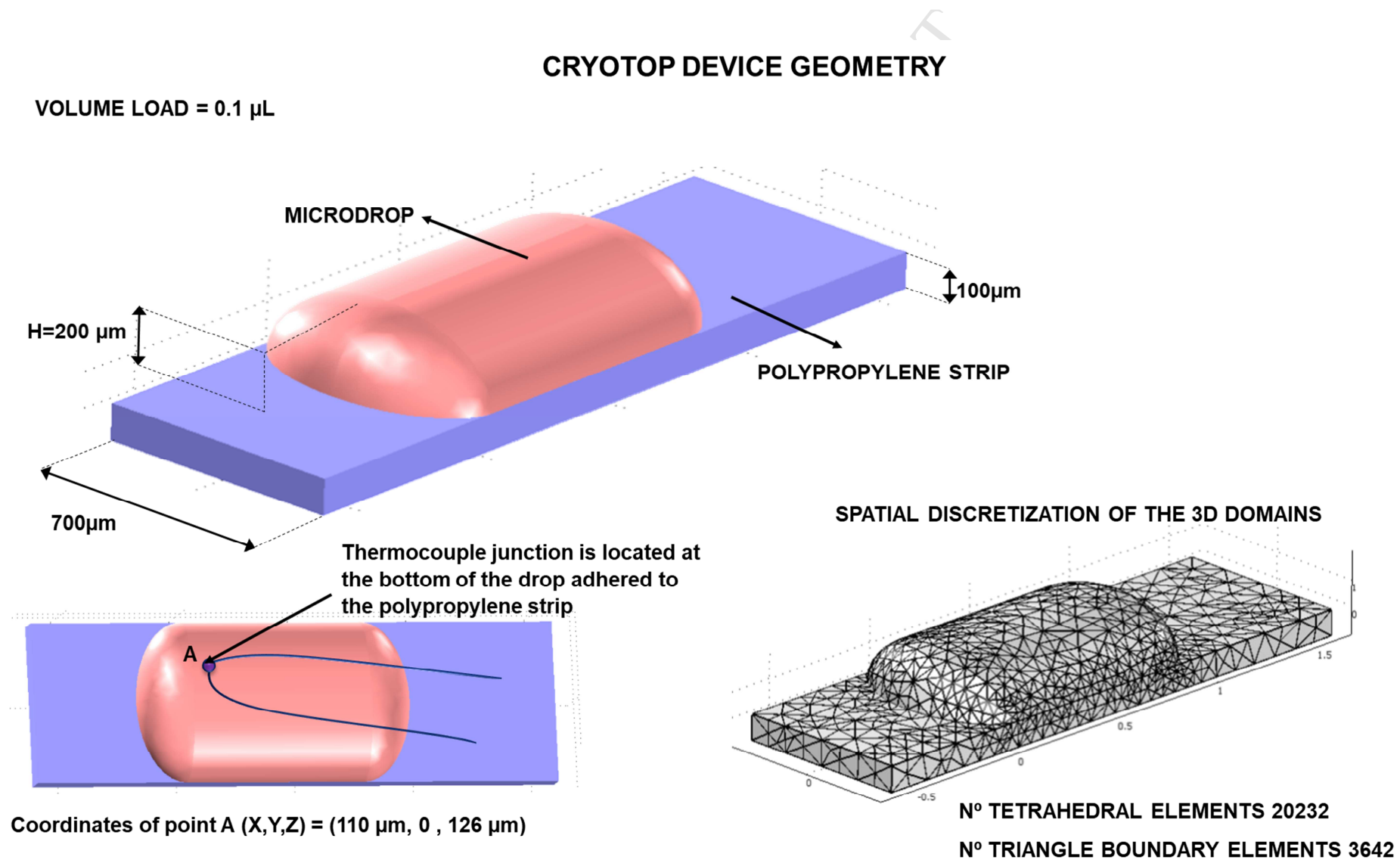


FIGURE 2

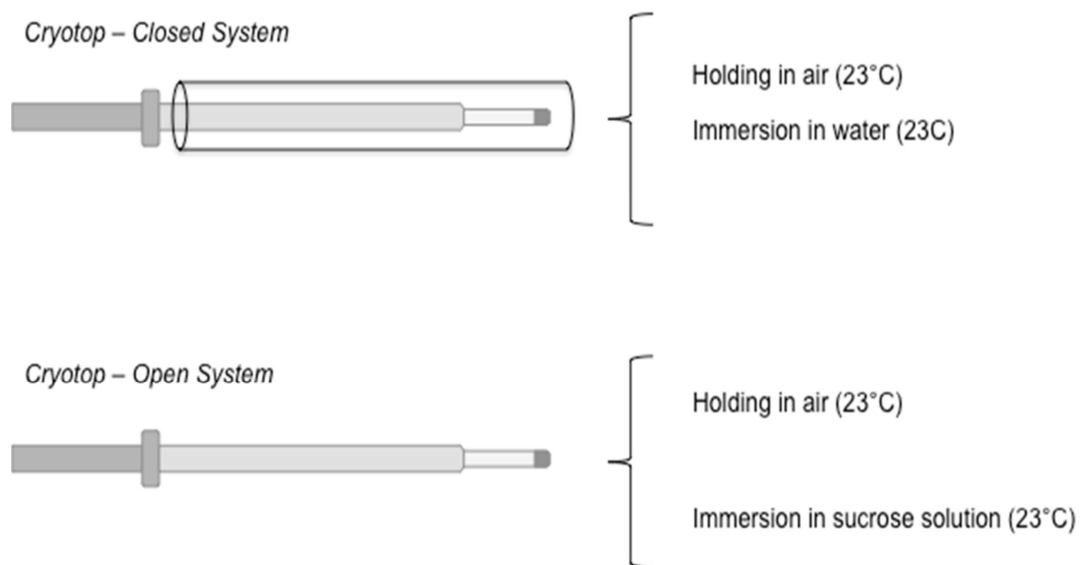


FIGURE 3

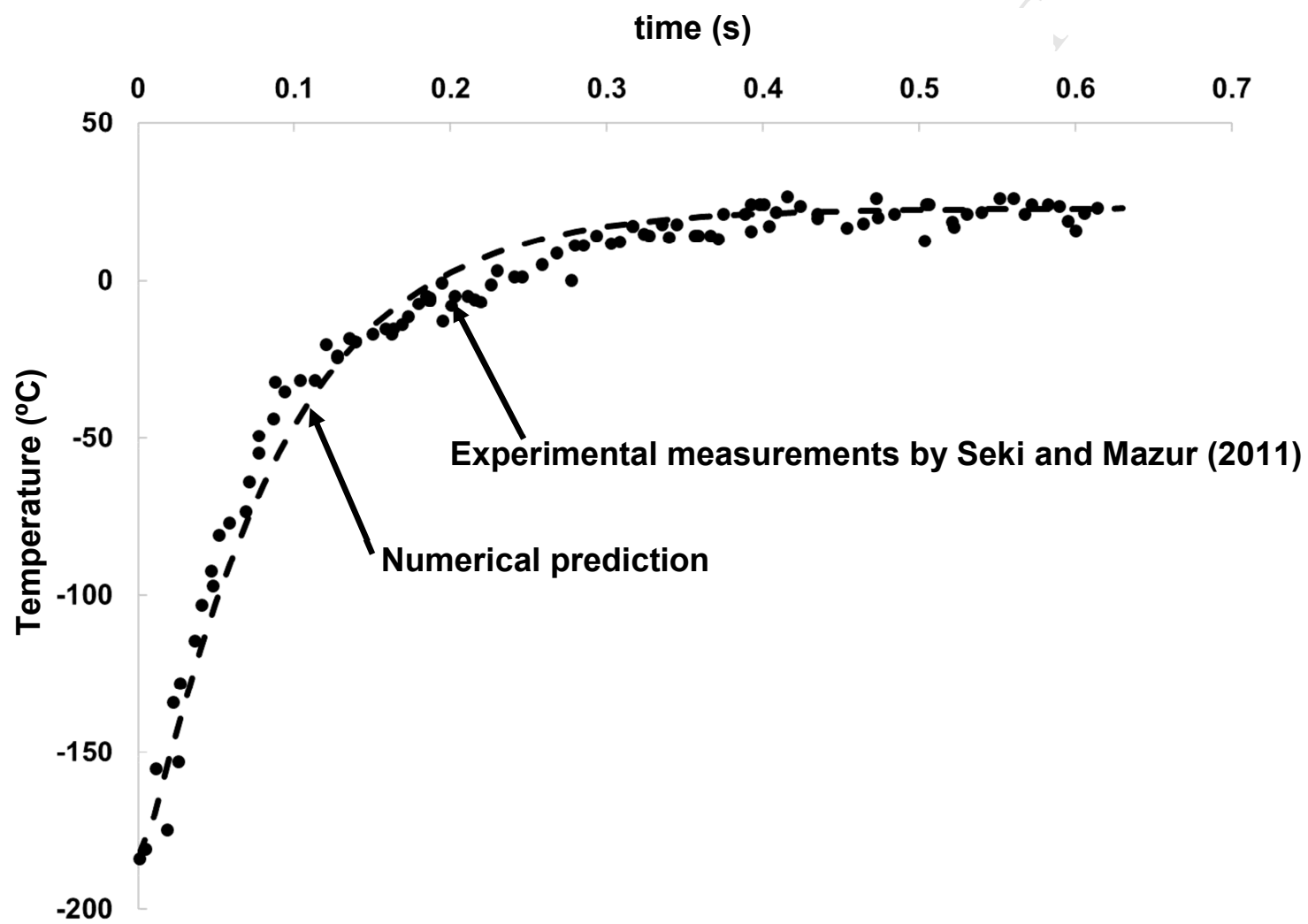


FIGURE 4

CRYOTOP DEVICE AFTER 0.1s IN WARMING SOLUTION

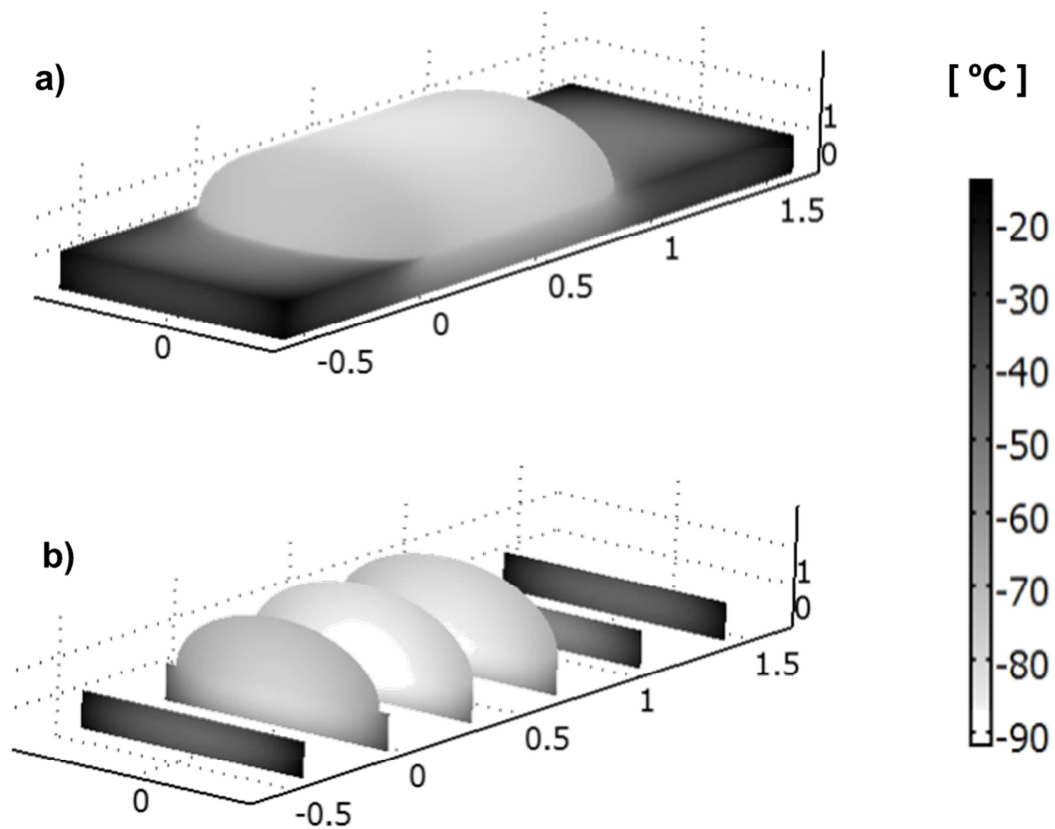
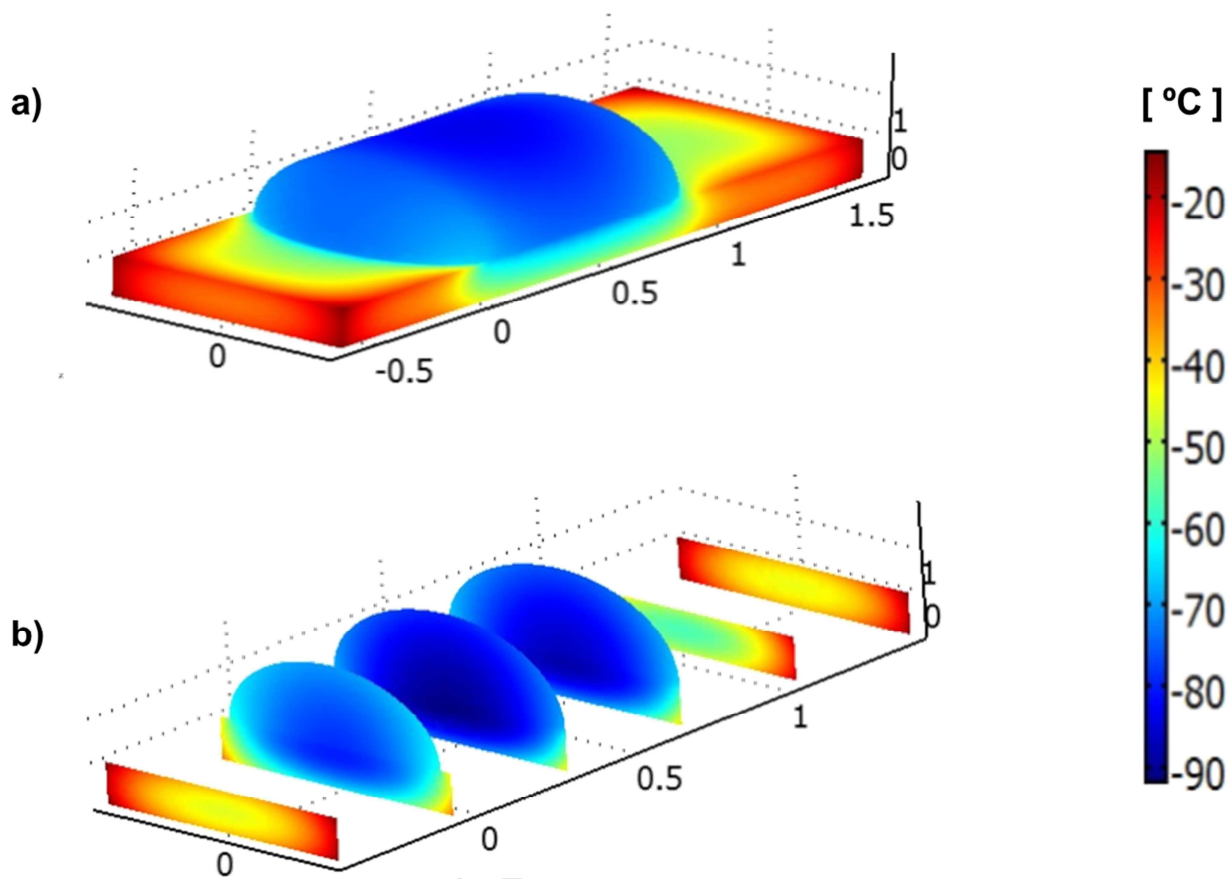


FIGURE 4

CRYOTOP DEVICE AFTER 0.1s IN WARMING SOLUTION



HIGHLIGHTS

Surface heat transfer coefficients of the Cryotop® during warming procedures

Mathematical modeling of heat transfer in Cryotop® during warming

Numerical simulations of the Cryotop® system using open and closed systems

ACCEPTED MANUSCRIPT

ROLE OF THE FUNDING SOURCE

The financial support for this research was provided by the following Institutions: 1) Facultad de Ciencias Agrarias, Universidad Católica Argentina (Ciudad Autónoma de Buenos Aires), 2) Centro de Investigación y Desarrollo en Criotecnología de Alimentos (CIDCA-CONICET-CIC PBA), 3) Universidad Nacional de La Plata (Bs As), 4) and Agencia Nacional de Promoción Científica y Tecnológica (ANPCYT). The funding sources had no involvement in the development and analysis of the results presented in the present work.